Supporting Information

Noble metal nanostructure as both SERS nanotag and analyte probe

Polina Pinkhasova, Benjamin Puccio, Tsengming Chou, Svetlana Sukhishvili and Henry Du**

Silver nanoparticles, Ag-Au nanoshells, and core-shell nanostructures

Figure 1S (1) shows a UV absorption spectrum of the solid Ag nanoparticles used for nanoshell and core-shell nanostructure synthesis with TEM image in inset. The nanoparticles had an average particle diameter of 47 ± 6 nm and ζ-potential of -48 mV (measured in Milli-Q water). Ag nanoparticles were aged in the fridge for one week and used as a template for nanoshell synthesis. UV absorption spectra on Figure 1S (2-6) shows a range of hollow nanoshells obtained with molar ratios of 20, 10, 8, 4, 3 and 2.85 of Ag^0 atoms in Ag nanoparticles to added $HAuCl_4$ with localized surface plasmon resonance (LSPR) ranging from 445 to 725 nm. The TEM image in inset corresponds to the nanoshell type (6) with LSPR at 668 nm. The nanoshells had an average particle diameter of 50 ± 6 nm and zeta-potential value of -17 mV (as determined using Zetasizer Nano-ZS), and atomic composition of 53% Au 47% Ag. These porous nanoshells with LSPR at 668 nm were used for the synthesis of label-free control and label-entrapped core-shell nanostructure.

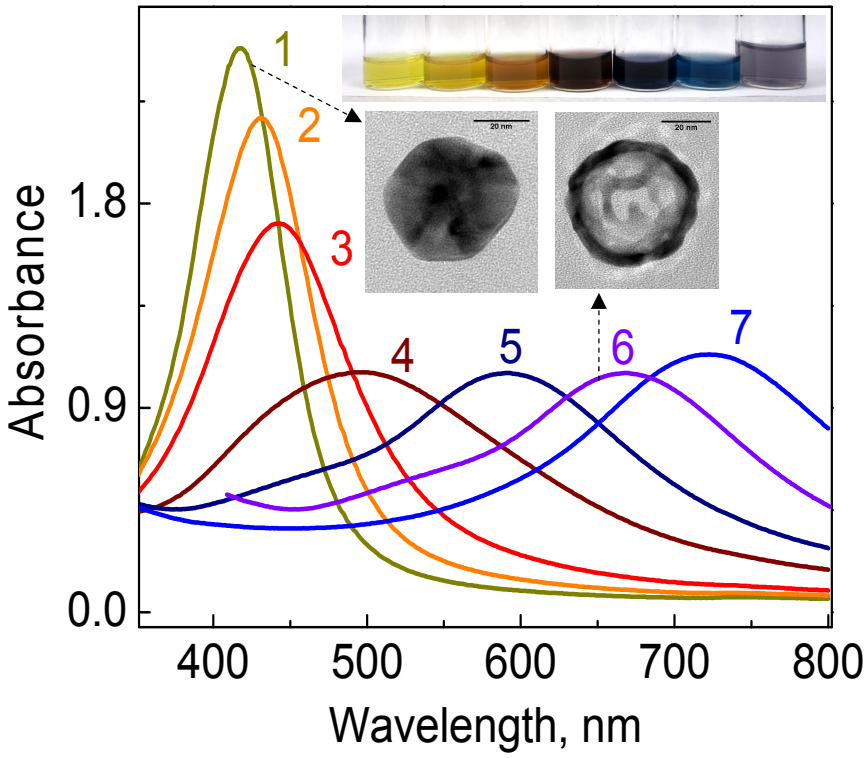

Figure 1S. UV-visible absorption spectra obtained for aqueous dispersions of (1) citrate-reduced Ag nanoparticles with LSPR of 408 nm, and (2-6) galvanic displacement reaction of porous alloyed Ag-Au nanoshells with molar ratios of 20, 10, 8, 4 and 2.85 of Ag^0 atoms in Ag nanoparticles to added $HAuCl_4$ with LSPR ranging from 445 to 725 nm. Insets show corresponding TEM images of (1) Ag nanoparticles with average diameter of 47 ± 6 nm and zeta-potential of -48 mV and (6) Ag-Au nanoshells with average diameter of 50 ± 6 nm and zeta-potential of -17 mV, and LSPR at 668 nm.

Figure 2S shows TEM images of nanoshells with LSPR at 668 nm with average particle diameter of 50 ± 6 nm and zeta potential of -17 mV. Shell thickness of the alloyed Ag-Au nanoshell of 5-8 nm and pore diameter of 5-12 nm was estimated from HR-TEM images.

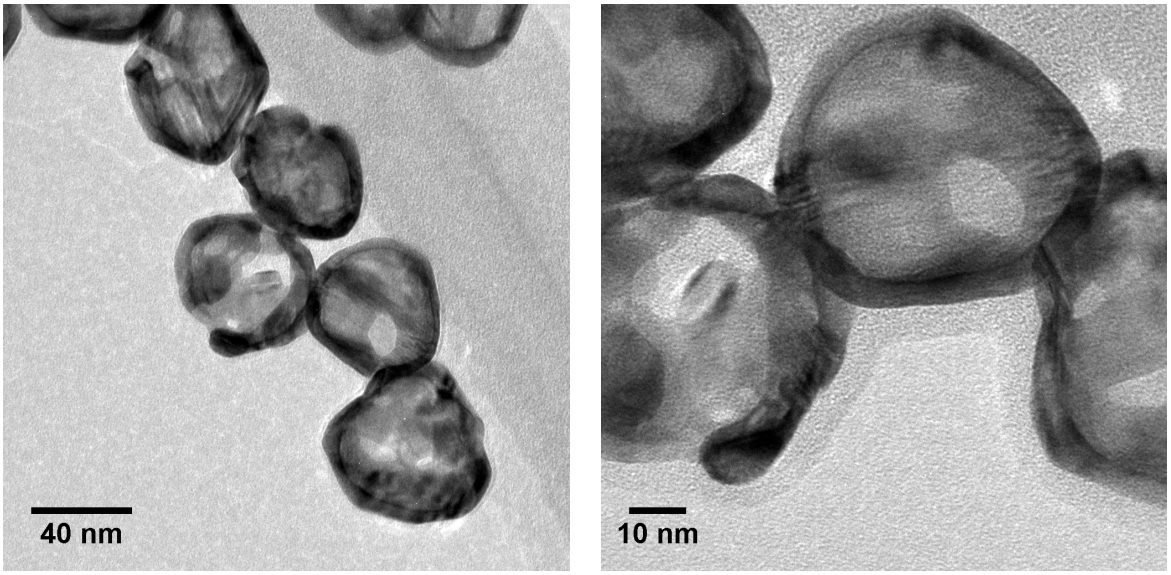

Figure 2S. TEM images of nanoshells with LSPR at 668 nm, with overall diameter of 50 ± 5 nm, shell thickness of 5-8 nm and 5-12 nm pores.

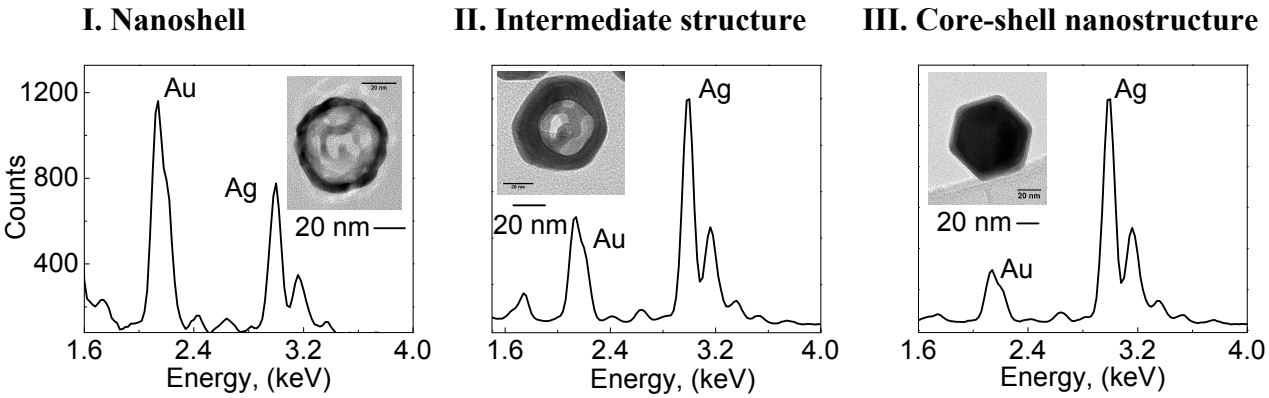

Figure 3S. EDX of nanostructures at various stages of core-shell nanostructure formation. (I) Porous Ag-Au nanoshells with average atomic composition of 53% Au and 47% Ag, (II) partially filled nanoshells with average atomic composition of 32% Au and 68% Ag (obtained by the addition of $3x10^{-7}$ moles of $AgNO_3$ and sodium citrate to a solution with 10^{12} nanoshells), and (III) core-shell nanostructure in the absence of the label molecule, resulting from complete filling of the hollow core of the nanoshell by citrate-reduced Ag with average atomic composition of 14% Au and 86% Ag (obtained by the addition of $2x10^{-6}$ moles of $AgNO_3$ and sodium citrate to a solution with 10^{12} nanoshells).

Control experiments:

Au nanoparticle synthesis

Au nanoparticles were prepared in a similar fashion to Ag nanoparticles. 4 mL of 1% aqueous sodium citrate was added to 40 mL of 5 mM $HAuCl_4$ solution. The mixture was placed under UV lamp for 30 min under constant stirring. Solution was maroon in color with LSPR peak at 520 nm. The nanoparticles had an average particle diameter of 85 ± 6 nm and zeta-potential of -40 mV.

Further reduction of $AgNO_3$ in the presence pre-formed citrate-reduced Ag and Au nanoparticles

10 mL of citrate reduced Ag nanoparticles with 10^{12} particles mL^{-1} (synthesized as described above) was boiled and 1 mL of 10 mM $AgNO_3$ with 1 mL of 1 % citrate was added. The solution was boiled for 10 minutes (or until the change in color was stable). Figure 4S below shows that original size of Ag nanoparticles stayed the same, instead of Ag growth on the surface of Ag nanoparticles after introduction of $2x10^{-6}$ moles of $AgNO_3$ and citrate in excess, nucleation and growth of new Ag nanoparticles took place. SEM image on the right shows that distinct facets were created on spherical Ag nanoparticles and growth of new shapes such as rods occured. Table 1S below shows dynamic light scattering (DLS) experiment for solid Ag nanoparticles upon introduction of $AgNO_3$ and citrate. Once again addition of $AgNO_3$ and citrate to Ag nanoparticles resulted in new growth of Ag as evident from an increase in polydispersity index and emergence of a new 11. 7 nm peak (number average size). Polydispersity index increased from 0.161 to 0.427 due to the appearance of this new peak of 11.7 nm. During UV assisted synthesis of Ag nanoparticles, citrate anions undergo photochemical and thermal oxidation resulting in products such as acetonedicarboxylic acid and acetoacetic acid, which adsorb to nanoparticle surface and prevent further growth of Ag. Table 1S shows that when citrate-reduced Ag nanoparticles were coated with PVP, the evolution in the nanoparticle size and distributions after addition of

$AgNO_3$ and citrate was the same as in the case of PVP-free citrate-reduced Ag nanoparticles. PVP partially displaces citrate products, and further prevents the growth of new Ag on PVP coated citrate-reduced Ag nanoparticles.

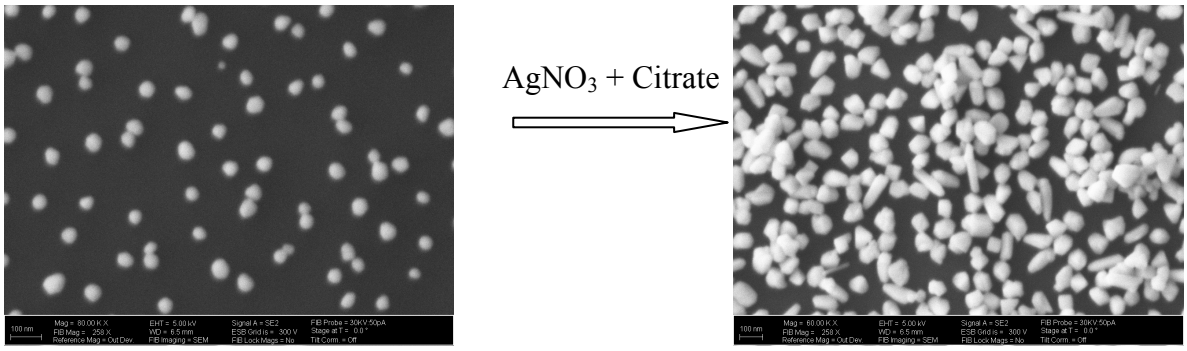

Figure 4S. SEM images of citrate reduced Ag nanoparticles as synthesized (left) and after addition of $2x10^{-6}$ moles of $AgNO_3$ and excess amount of citrate to 10^{12} particles mL^{-1} of pre-formed Ag nanoparticles (right).

Table 1S. Dynamic light scattering measurements (hydrodynamic radii (R_H) and polydispersity indices) of citrate-reduced Ag nanoparticles, and citrate-reduced Ag nanoparticles coated with PVP, before and after the addition of $AgNO_3$ with citrate to induce further growth of silver. R_H 1 and R_H 2 refer to R_H's of two fractions of particles as identified by Malvern software.

Nanoparticles	***R_H* 1 (nm)**	***R_H* 2 (nm)**	**PDI**
Ag NPs	49.28 (100 %)*	0	0.161
Ag NPs after addition of $AgNO_3$ and citrate	41.23 (85%)	11.7 (15%)	0.427
Ag NPs coated with PVP	71.78 (100%)	0	0.141
Ag NPs coated with PVP after addition of $AgNO_3$ and citrate	75.82 (88%)	12.56 (12%)	0.303

*number in parentheses indicates the percentage of scattered intensity within peaks 1 and 2 as identified by Malvern software.

Similar experiments were done with citrate reduced Au nanoparticles. 10 mL of citrate reduced Au nanoparticles (synthesized as described above) was boiled and 1 mL of 10 mM $AgNO_3$ with 1 mL of 1 % citrate were added. The solution was boiled for 10 minutes (or until the change in color was stable). Similarly to experiments with Ag nanoparticles, the growth of Ag on Au nanoparticles did not take place as DLS data shows on Table 2S. Instead, silver independently nucleated and grew, while the size of Au nanoparticles remained unchanged.

Table 2S. Dynamic light scattering measurements (hydrodynamic radii (R_H) and polydispersity indices) of citrate-reduced Au nanoparticles, and citrate-reduced Au nanoparticles covered with PVP, before and after the addition of $AgNO_3$ with citrate to induce further growth of silver. R_H 1 and R_H 2 refer to R_H's of two fractions of particles as identified by Malvern software.

Nanoparticles	**R_H 1 (nm)**	**R_H 2 (nm)**	**PDI**
Au NPs	104.4 (100 %)	0	0.153
Au NPs after addition of $AgNO_3$ and citrate	119.5 (91.3%)	942 (8.7%)	0.362
Au NPs coated with PVP	129.6 (100%)	0	0.115
Au NPs coated with PVP after addition of $AgNO_3$ and citrate	138.5 (96%)	854 (4%)	0.271

*number in parentheses indicates the percentage of scattered intensity within peaks 1 and 2 as identified by Malvern software.

Nanotags

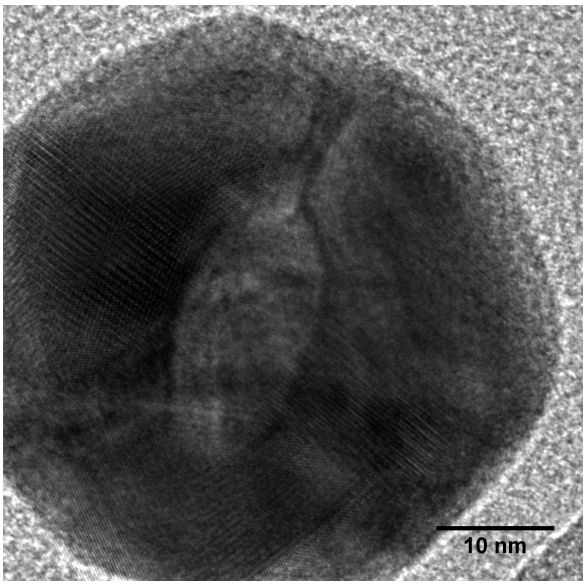
10 nm

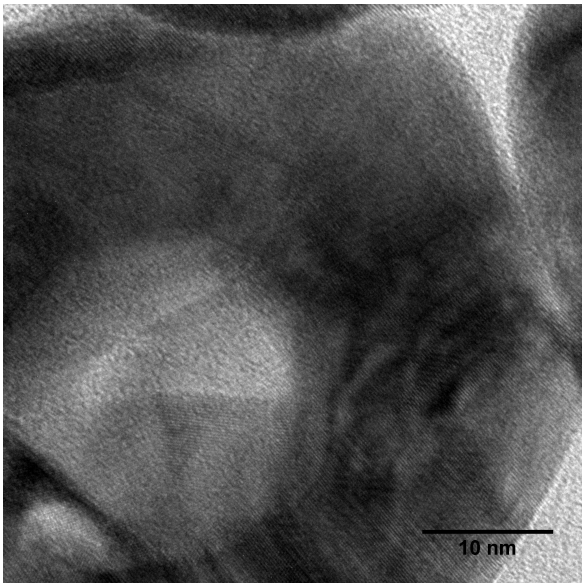
10 nm

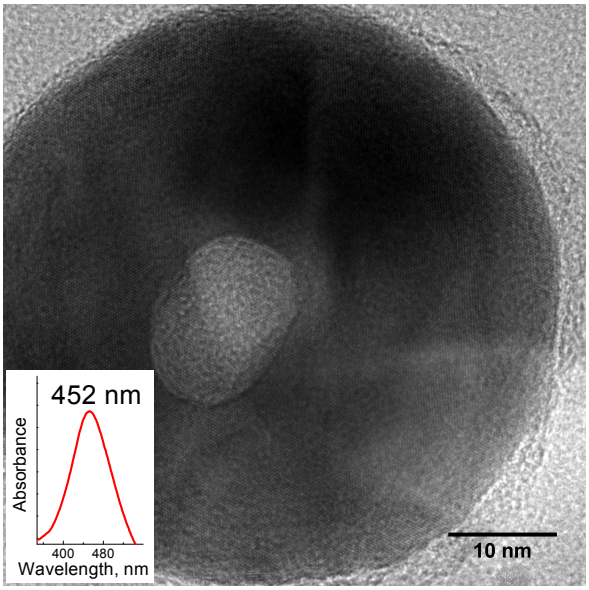
452 nm
Absorbance
400
480
Wavelength, nm
10 nm

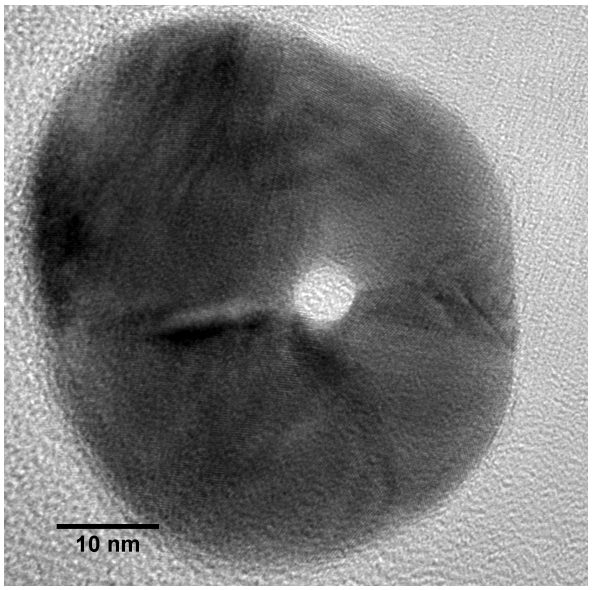
10 nm

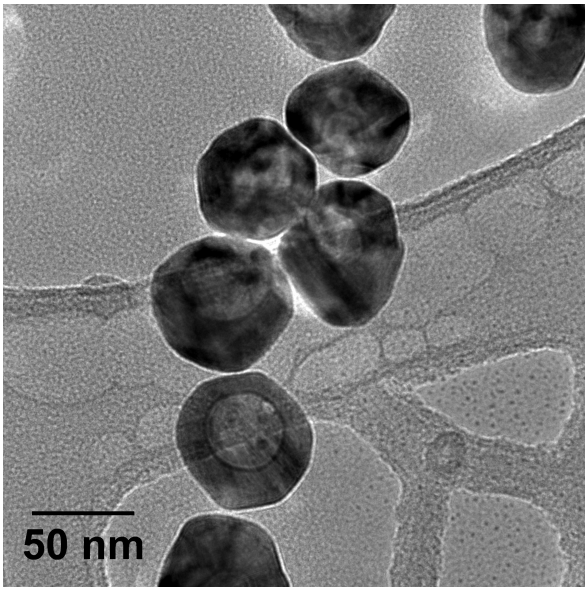
50 nm

Figure 5S. HR-TEM images of nanotags with LSPR at 452 nm, loaded with SCN- label. Average particle diameter of 50 ± 6 nm and ζ-potential of -17 mV remained the same as that of nanoshells, and the pore size of 5 to 15 nm was estimated from HR-TEM images.

SERS activity of nanostructures

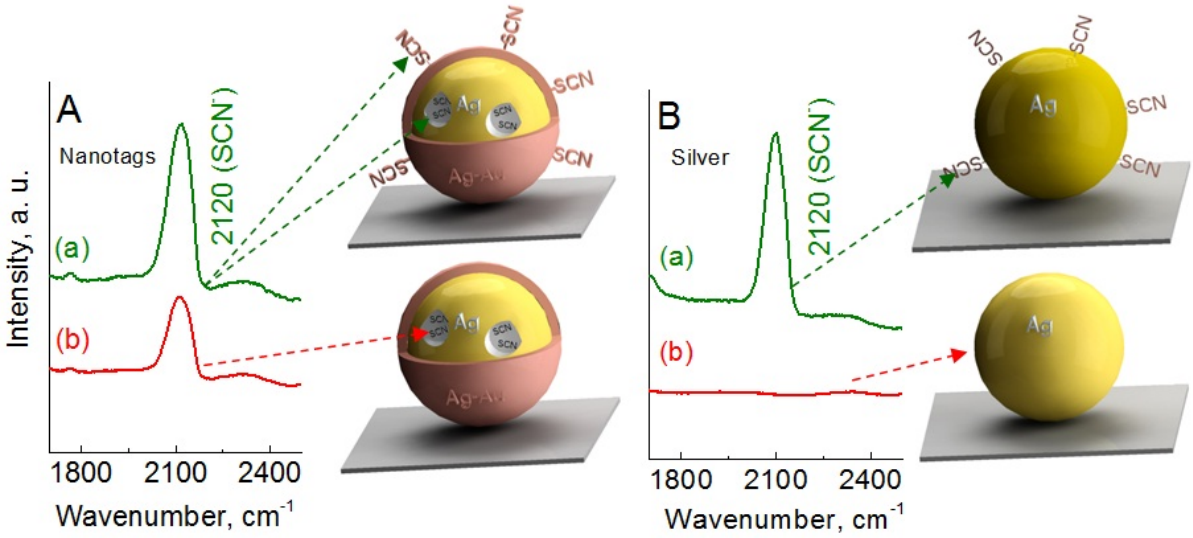

Figure 6S. SERS activity of immobilized nanostructures on silicon substrate. SERS spectra of (A-a) nanotags loaded with SCN^- both within and on the surface of the nanostructure with coverage density of ~80 particles/μm^2, (A-b) nanotags treated with 0.1 M NaCl that displaced surface-adsorbed SCN^-. (B-a) SCN^- adsorbed at the surface of Ag nanoparticles with coverage density of ~75 particles/μm^2, (B-b) after subsequent treatment with 0.1 M NaCl. Raman spectra were acquired at an excitation wavelength of 633 nm (4 mW, and exposure time of 20 s).

SEM images of SERS substrates

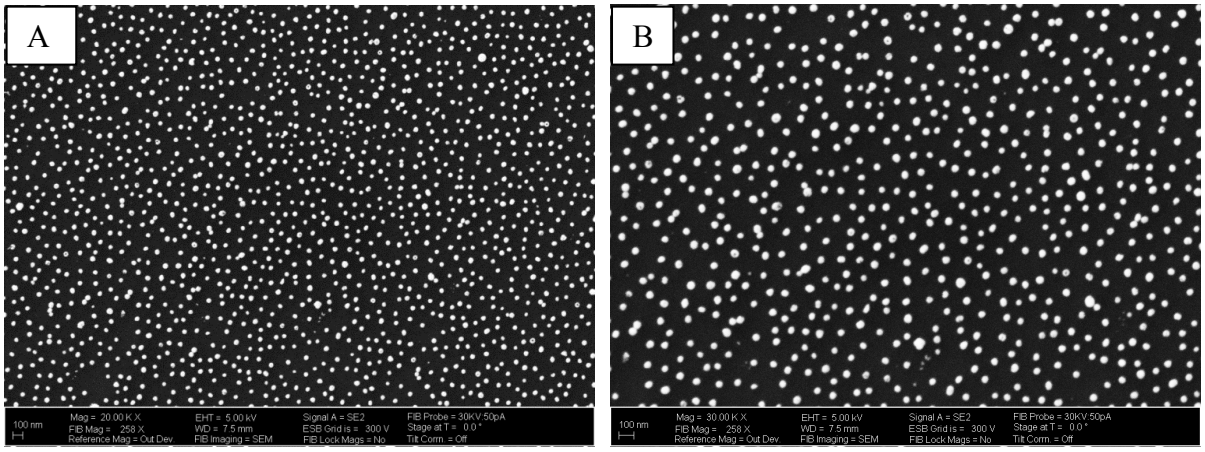

Figure 7S. SEM images of nanotags with ~80 particles/μm^2 immobilized at the surface of silicon and used as a SERS substrate (A) as synthesized and (B) after subsequent treatment with 0.1 M NaCl.

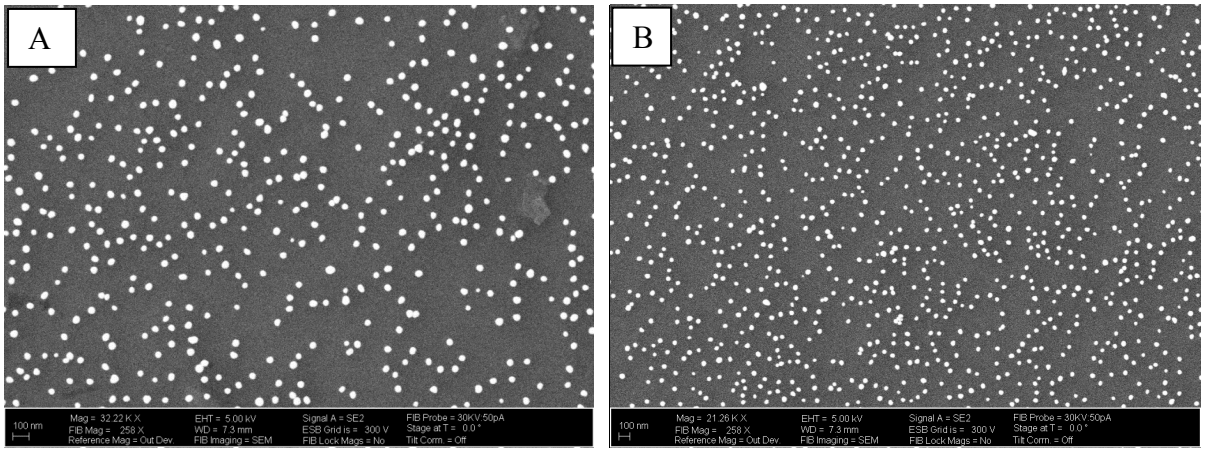

Figure 8S. SEM image of citrate-reduced Ag nanoparticles with ~75 particles/μm^2 immobilized at the surface of silicon and used as a SERS substrate (A) as synthesized and (B) after subsequent treatment with 0.1 M NaCl.

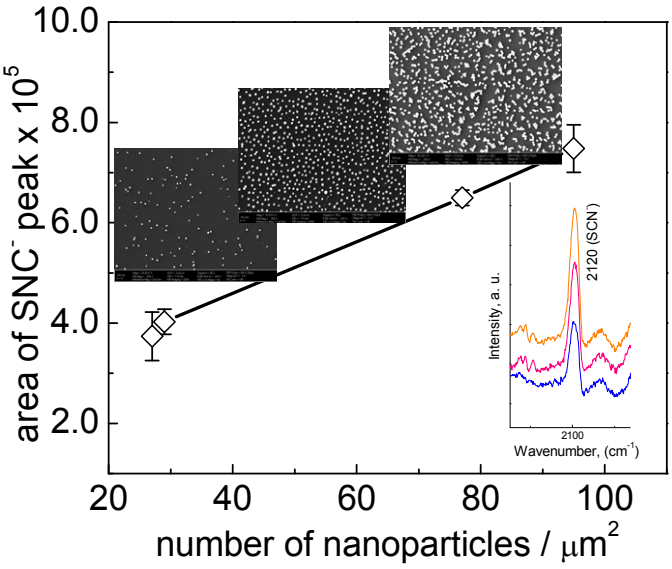

Figure 9S. Linear correlation between SERS intensity of SCN^- band and nanoparticle coverage density as supported by SERS and SEM measurements. Raman spectra were acquired at an excitation wavelength of 633 nm (4 mW, and exposure time of 20 s).

SERS substrate used for imaging and SERS measurements

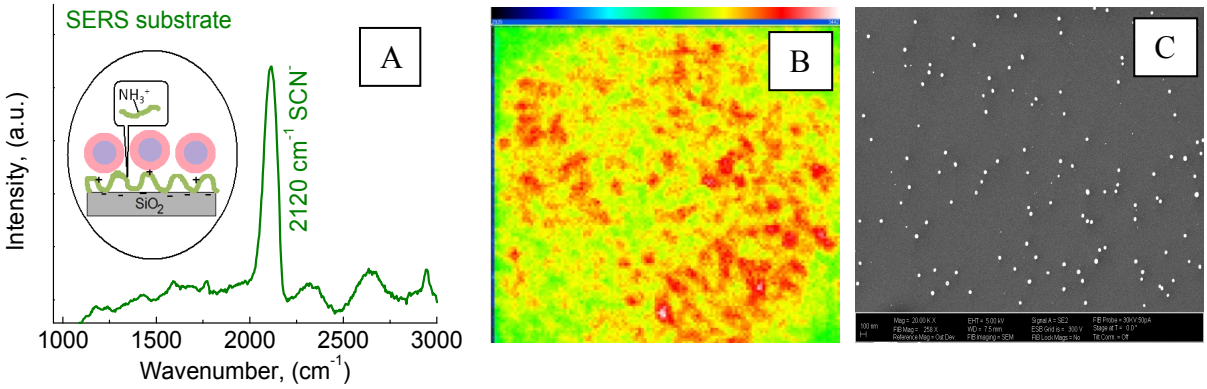

Figure 10S. SERS spectrum of core-shell nanostructure with characteristic SCN^- vibration at ~2120 cm^{-1} (A) and corresponding Raman and SEM images (B and C, repectively). SERS spectrum (A) and Raman image were acquired at an excitation wavelength of 633 nm (20 mW, and exposure time of 20 s). Inset in SERS spectrum (A) shows a schematic representation of immobilization process through electrostatic interaction of the positively charged PAH surface with the negatively charged nanoparticles.

Experiment Section

Materials: The following reagents were purchased from the indicated suppliers and used without further purification: silver nitrate (ultrapure grade, Across), sodium chloride (99.999%, Sigma), sodium citrate (Fisher), hydrogen tetrachloroaurate (III) (30 wt% solution in dilute hydrochloric acid, 99.999%), poly(vinyl pyrrolidone) (PVP) (weight-average molecular weight of 40,000 g mol^{-1}, Sigma), poly (allylamine hydrochloride) (PAH) (weight-average molecular weight of 15,000 g mol^{-1}, Aldrich), 1,2-di-(4-pyridyl)ethylene (BPE) (Sigma), sodium thiocyanate (SCN^-) (99.99+%, Sigma). All glassware was cleaned in nochromix solution and sulfuric acid for 24 hours, followed by thorough washing with Milli-Q water.

Synthesis of Silver: Ag nanoparticles were synthesized by a modified Lee and Meisel method[16] with aid of UV irradiation, details of which can be found elsewhere.[17] Briefly, 1% aqueous sodium citrate (0.8 mL) was added to $AgNO_3$ solution (100 mM, 40 mL). The mixture was placed under a UV lamp (UV Flood Curing System, Cure Zone 2 (CON-TROL-CURE, Chicago, IL)) for 4 hours with gentle stirring. Figure 1S (1) shows a UV absorption spectrum of the Ag nanoparticles with TEM image in inset. The nanoparticles had an average particle size of 47 ± 6 nm and zeta-potential of -48 mV. Ag nanoparticles were aged in the fridge for one week and used as a template for nanoshell synthesis.

Synthesis of Silver-Gold Nanoshells: Au-Ag hollow nanoshells were obtained via galvanic replacement reaction,[18] using Ag nanoparticles as a template. A 10 mL mixture of Ag nanoparticles (0.3 mM) and PVP (1 mg mL^{-1}) was heated to boil. Immediately upon boiling a specific amount of aqueous $HAuCl_4$ (0.5 mM) was added dropwise under stirring, with a colloidal Ag to $HAuCl_4$ molar ratio ranging from 2.85 to 20 in the solution mixture. The color changed instantly. The solution was boiled for another minute to ensure completion of reaction as evidenced by color stabilization. Once cooled to room temperature, the resultant nanostructures were centrifuged two times (under 5,000 RPMS for 5 minutes) and washed

with Milli-Q water to remove silver chloride by-product and free PVP. Figure 1S (2-6) shows the UV absorption spectra of hollow nanoshells with localized surface plasmon resonance (LSPR) ranging from 445 to 725 nm. The TEM image in inset corresponds to nanoshell with LSPR at 668 nm. The nanoshells had an average particle size of 50 ± 6 nm and zeta-potential value of -17 mV. Porous nanoshells with LSPR at 668 nm were used for the synthesis of Ag core/Au-Ag nanoshells with and without label molecules.

Synthesis of Core-Shell Nanostructure: Core-shell nanostructures without and with entrapped SCN^- label molecules were synthesized, starting from Ag-Au porous nanoshells with average atomic composition of 53% Au and 47% Ag and localized surface plasmon at 668 nm. Synthesis of the control core-shell nanostructure with maximal amount of filled core with Ag was conducted by the addition of excess $AgNO_3$: 10 mL of porous Ag-Au nanoshells (10^{12} particles mL^{-1}) were brought to a boil, next 200 µL of 100 mM $AgNO_3$ were added in a drop way fashion followed by 0.8 mL of 1% aqueous sodium citrate. The color of the blue solution turned to yellow immediately after addition of $AgNO_3$ and sodium citrate. The solution was boiled for another 10 minutes to insure completion of the reaction. Intermediate core-shell nanostructure shown on Figure 1(II) was synthesized by the addition of limited amount of $AgNO_3$ to nanoshell: 10 mL of porous Ag-Au nanoshells (10^{12} particles mL^{-1}) were brought to a boil, and 30 µL of 10 mM $AgNO_3$ were added in a drop way fashion followed by 0.8 mL of 1% aqueous sodium citrate. Core-shell nanostructure with entrapped SCN^- was synthesized as follows: porous Ag-Au nanoshells were mixed with SCN^- to obtain a final volume of 10 mL with nanoshell concentration of 10^{12} particles ml^{-1} and final SCN^- concentration of 10^{-6} M. This solution was mixed overnight under gentle stirring, next the solution was brought to a boil and 200 µL of 100 mM $AgNO_3$ were added in a drop way fashion followed by 0.8 mL of 1% aqueous sodium citrate. The resultant nanotags were centrifuged two times (under 5,000 RPMS for 5 minutes) and washed with Milli-Q water to remove extra SCN^-.

Characterization of Nanostructures: The size and distribution, surface charge, and plasmon resonance of the resultant nanostructures were determined by transmission electron microscopy (TEM, Philips CM20), scanning electron microscopy (Auriga Ziess Dual-Beam SEM), dynamic light scattering and laser doppler microelectrophoresis (Zetasizer Nano-ZS, Malvern Instruments), and UV-visible absorption spectroscopy (Synergy HT Multi-Detection Microplate Reader, BioTek Instruments). All high resolution-transmission microscopy data was collected using JEOL 2100F at Brookhaven National Laboratory, and analysis was done using Gatan-DigitalMacrograph software. Atomic composition of nanoshells and core-shell nanostructures was determined by EDX with elemental mapping using Philips CM 20 TEM.

SERS measurements: For all SERS substrates, nanostructures (Ag NPs, Ag-Au nanoshells, or nanotags) were immobilized in a controlled fashion on a silicon substrate.[8] [14]Briefly, silicon substrate was immersed in aqueous solution of PAH (2 mg ml^{-1}) at pH 9 for 20 minutes to allow polymer adsorption to the surface. Next, this substrate was rinsed with Milli-Q water at pH 4.5 to remove any free or loosely bound PAH. Nanostructures were attached to the PAH modified surface using a solution of 10^{12} particles ml^{-1} for 4 hours. Nanostructures were immobilized through electrostatic interaction of the positively charged PAH surface with the negatively charged nanostructure surface as well as via the binding affinity of Ag and Au to amino groups in PAH. SERS measurements were conducted using 632.8 nm excitation wavelength using a custom built Raman setup, described in detail elsewhere.[19] To ensure statistical significance, SERS measurements were done on three identically prepared of the same nanostructure type, and five measurements were done on each of those substrates; variations between identically prepared substrates and spot-to-spot variation were less than 10%. All SERS data were processed using Origin 8.0 software.